THE ARCHIVE OF MECHANICAL ENGINEERING

VOL. LV 2008 Number 4

DOI: 10.24425/ame.2008.131634

Key words: welded joints, Vickers indentation, fatigue crack, crack initiation, fatigue strength

VLADIMIR GLIHA [*], *VOLODYMYR HUTSAYLYUK* [**], *LUCJAN SNIEZEK* [**], *TOMAZ VUHERER* [*]

MODELLING FATIGUE CRACK GROWTH IN HAZ OF WELDED AREA

The small artificial surface defects in the coarse-grain steel are studied. The size of the used defects is smaller than the most relevant microstructural unit of steel, i.e. the average grain size. The samples of coarse-grain steel are prepared using a welding thermal-cycle simulator and a laboratory furnace. The defects are made by indenting with a Vickers pyramid. One of the final results of the defect making is the existence of local residual stresses. The influence of residual stresses on the crack initiation from those artificial defects is discussed in the article.

1. Introduction

Defects decrease fatigue strength of metals. In the past, S-N curves were the only available tool to predict the fatigue lives of defected metals. Now, LEFM concepts are often applied to the cracks which do not belong to microstructurally small cracks.

Murakami and co-workers treated the influence of small defects of various shapes in the same way as cracks, i.e. using LEFM concepts [1-3]. Square root of the defect projection onto the plane that is perpendicular to the cyclic stress is a parameter reflecting the effect of small defects on fatigue strength of metallic materials. However, LEFM greatly underestimates the propagation rates of short cracks within the local plastic zones that develop as a result of stress concentration [4, 5].

[*] *University of Maribor, Faculty of Mechanical Engineering, Institute for Engineering Design, Smetanowa 17 St., Maribor, 2000, Slovenia, E-mail: vladimir.gliha@uni-mb.si*

[**] *Military University of Technology, Faculty of Mechanical Engineering, Department of Machine Design, Gen. S. Kaliskiego 2. St., 00-908 Warsaw, Poland, E-mail: l.sniezek@wme.wat.edu.pl*

Cracks much smaller than the smallest microstructural units have no influence on the fatigue strength of metals. The cracks initiated from small defects propagate at the beginning unexpectedly fast. The propagation decelerates gradually when the tip of a crack approaches microstructural obstacles such as grain boundaries. The propagation even stops, and cracks become non-propagating. However, in the presence of cracks whose size is comparable to the microstructural units of the metal, the fatigue strength is lowered. The behaviour of metals with cracks of different size, from the smallest ones (short cracks), over medium ones (physical small cracks) to the biggest ones (long cracks), can be successfully described using the Kitagawa-Takahashy diagram [6].

Each weld consists of base material, heat affected zone (HAZ) and deposited metal. The filler material and a part of the base material melt down during welding and form the solidified weld metal, while the base material in the close vicinity undergoes a remarkable microstructural change.

The HAZ formation is the result of an applied thermal cycle caused by the movement of the heat source. The heat is needed for melting a sufficient quantity of welded and filler materials. The effects of thermal cycles diminish with the distance from the fusion line. The material adjacent to the fusion line is, for some time, heated almost to the melting point. The result is an extensive grain growth. In this area, the microstructure of a coarse-grain heat-affected zone (CGHAZ) is formed. Mechanical properties, such as impact toughness and fatigue limit, are always defined by the microstructure, which is drastically changed in the course of weld manufacturing.

Due to the shape of solidified weld metal, a concentration of stress appears at the weld toes of mechanically loaded welds. In order to avoid stress concentration, fine grinding of the weld reinforcement can be performed, although it is economically hardly acceptable. If grinding is not carried out, the fatigue strength of the welded joints is certainly reduced due to the concentrated cyclic stress.

Small defects are always present in metals due to the way of their processing. Weld defects in the weld metal and HAZ appear mainly due to the insufficiently controlled welding process. The NDE methods are used in the industry to ensure soundness of welds. The defects that are smaller than the threshold sensitivity of the NDE method cannot be detected. Defects promote crack initiation during the cyclic loading. The final consequence of the defect presence is lower fatigue strength of welds.

During the cyclic loading, fatigue cracks will appear if the stress amplitude is sufficiently high. The first stage of the fatigue crack appearance is crack initiation. When micro-defects are present, the crack initiation is easier because of locally less convenient stress/strain field. When the size of the

defects is smaller than the biggest microstructural units, the effect of defects on the fatigue limit of metals is negligible.

So, the possibility of crack initiation at the weld toe is of greatest importance for the load-carrying capacity of cyclically loaded welded structures (Figure 1). Small weld defects, such as sharp transitions, different inclusions, scratches or cracks, are often present at the weld toe. Because of concentrated stress at the toes, cracks initiate in the coarse-grain steel that belongs to the CGHAZ [7].

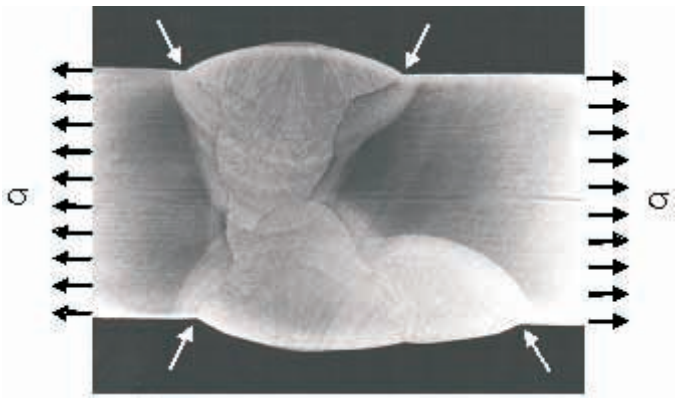

Fig. 1. Macrograph of a K-butt weld with a remote homogeneous stress. The arrows indicate the weld toes, the positions of concentrated stress field

According to Murakami [1 3], the fatigue limit, σ_w, of polycrystalline metals with small defects and the threshold stress intensity factor, ΔK_{th}, defining condition for macroscopic cracks development from small defects are calculated from the parameter $\sqrt{\text{area}}$ and hardness HV as:

$$\sigma_w = \frac{1.43(HV + 120)}{\left(\sqrt{\text{area}}\right)^{\frac{1}{6}}} \quad ; \quad \Delta K_{th} = 3.3 \cdot 10^{-3} (HV + 120) \cdot \left(\sqrt{\text{area}}\right)^{\frac{1}{3}} \quad (1)$$

σ_w is expressed in MPa, ΔK_{th} in MPa $m^{1/2}$, HV in the hardness number, $\sqrt{\text{area}}$ in μm.

The effects of small weld defects in the CGHAZ can be modelled by using artificial defects. Especially, small holes have been used in the past with great success in the studies of effects of small defects on the endurance limit of metallic materials. The use of small defects made by Vickers indenter is very promising for experimental research. Namely, the preparation of indentation at a prescribed size is very easy to execute, because only the data of material hardness are necessary. A problem with the use of Vickers indentations as the artificial weld defects are the residual stresses. Any kind of defects made

in mechanical way results in the appearance of residual stresses. The reason is irreversibility of plastic deformation, which is very extensive in the case of indenting with the Vickers pyramids. High residual stresses affect the local stress/strain conditions and change the actual shape of Vickers indentation.

The behaviour of coarse-grain steels with different types of microstructurally small defects in stress concentrated condition is studied in the present article. Defects are prepared by Vickers indenters.

2. Experimental works

In the first part of the present experimental work, samples of coarse grained HAZ steels in the as-welded condition were prepared by simulating thermal conditions during welding close to the weld. Slovene HSLA structural steel, grade HT 80, was used. Chemical composition of the steel and its basic mechanical properties in the quenched and tempered condition are shown in Table 1.

Table 1.

Chemical composition and properties of the structural steel

C	Si	Mn	P	S	Cr	Ni	V	Al	Ti
mass %									
0.09	0.27	0.3	0.015	0.01	1.05	2.63	0.07	0.045	0.026
$R_{0.2}$ [MPa]		R_m [MPa]		A_5 [%]			CVN [J], -40°C		
713		764		17			170		

The complete results of this research can be found elsewhere [8]. Welding thermal-cycle simulator was used to prepare samples of different kinds of coarse-grain steels. The microstructure was either pure martensitic (M) or martensitic with small portion of bainite (M+B). Five different types of the simulated coarse-grain HAZ microstructures are designated as M1-M5. They were formed in the range of cooling from $\Delta t_{8/5} = 5$ to $\Delta, t_{8/5} = 9.5$ s. The data on the cooling times, the mechanical properties and the microstructure are shown in Table 2. Mark M denotes martensite while mark B bainite.

An example of thermal cycle simulation and its result when applying to the steel is shown in Figure 2.

The specimens for testing were machined from the samples with simulated CGHAZ microstructure. The shape and the size of the specimens are shown in Figure 3. They were notched in the region with the simulated HAZ microstructure. The bottom of the notch was ground and polished. The theoretical stress concentration factor caused by the notch was 1.74. The

Table 2.

Simulation parameters, mechanical properties, microstructures and test conditions

M1	Cooling time $t_{8/5}$ [s]	Yield strength $R_{0.2}$ [MPa]	Tensile strength R_m [MPa]
	5	981	1210
	Grain size d [μm]	Micro-structure	Condition
	130	M	C_1,C_2,C_3,C_4,C_6
M2	Cooling time $\Delta t_{8/5}$[s]	Yield strength $R_{0.2}$[MPa]	Tensile strength R_m[MPa]
	9	935	1171
	Grain size d [μm]	Micro-structure	Condition
	140	M+B	C_1, C_2, C_4, C_6
M3	Cooling time $\Delta t_{8/5}$[s]	Yield strength $R_{0.2}$[MPa]	Tensile strength R_m[MPa]
	5.5	992	1192
	Grain size d [μm]	Micro-structure	Condition
	180	M	C_1, C_2, C_4, C_6
M4	Cooling time $\Delta t_{8/5}$[s]	Yield strength $R_{0.2}$[MPa]	Tensile strength R_m[MPa]
	9.5	939	1176
	Grain size d [μm]	Micro-structure	Condition
	140	M+B	C_1, C_2, C_4, C_5, C_6
M5	Cooling time $\Delta t_{8/5}$[s]	Yield strength $R_{0.2}$[MPa]	Tensile strength R_m[MPa]
	9.5	921	1172
	Grain size d [μm]	Micro-structure	Condition
	180	M+B	C_1, C_2, C_4, C_5, C_6

smooth surface at the bottom of the notch is specified as test condition C_1 in Table 2.

Small defects of different size and shape were made by a Vickers indenter at the bottom of the notch: single indentations, and series of five indentations in the straight line perpendicular to the testing stress.

The average size of single indentations, d, is 105, 160, and 221 μm. These situations are specified in Table 2 as test conditions C_2, C_3 and C_4. The average length of series of indentations, l, is 386 and 692 μm. These situations are specified in Table 2 as test conditions C_5 and C_6. The series were composed by indentations with diagonals approximately 110 and 220 μm.

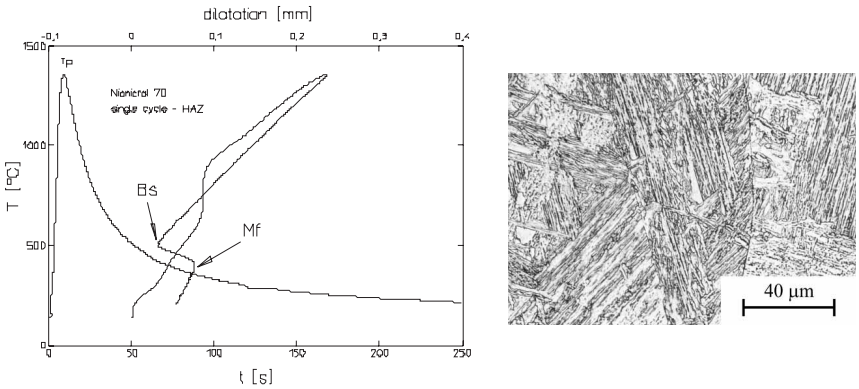

Fig. 2. Thermal cycle and dilatometric curve registered during the simulation of CGHAZ microstructure on the structural steel (left), formed CGHAZ microstructure (right)

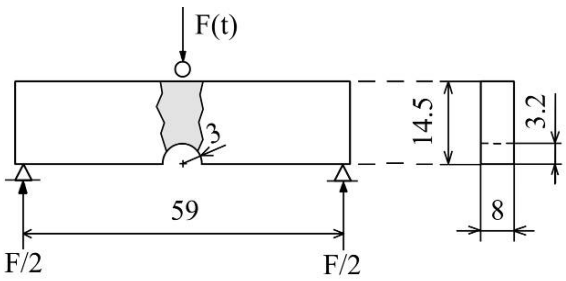

Fig. 3. Bend specimen with the notch positioned in the material with the simulated microstructure

The depth of the artificial defects is necessary to evaluate the parameter $\sqrt{area}$. Assuming the size of indentation dependent only on the length of the diagonal, we don't take into account the local residual stresses caused by irreversible material deformation. The angle between the opposite planes of the Vickers pyramid is 136°. The angle, α, between the opposite edges that form the diagonal is bigger, and the depth, b, is expressed as follows:

$$\alpha = 2\text{arctg}\left(\sqrt{2}\cdot \text{tg}\frac{136^\circ}{2}\right) \quad ; \quad b = \frac{d\sqrt{2}}{4}\cdot \text{ctg}\frac{136^\circ}{2} \tag{2}$$

The defect size parameter $\sqrt{area}$ is evaluated for each of the used artificial defects, the single indentations of three sizes and the series of indentations in two sizes. A special approach for the evaluation of long-shallow small defects is available [9].

As shown in Figure 4, the *area* is a plane of the actual defect projection for the single indentation and the product of the maximum defect width with the length of ten times the depth for the series of indentations [9]:

$$area|_{\text{ind}} = \frac{d^2\sqrt{2}}{8}\text{ctg}\frac{136^\circ}{2} \quad ; \quad \text{area}|_{\text{series}} = \frac{5d^2\sqrt{2}}{4}\text{ctg}^2\frac{136^\circ}{2} \tag{3}$$

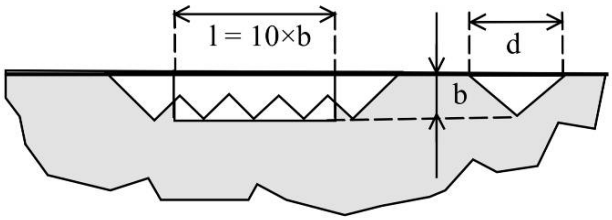

Fig. 4. Size of the parameter *area* calculated for the single indentation and the series of indentations

In the second part of the present experimental work, the coarse-grain steel was prepared with heat treatment in furnace, as shown in Figure 5. Slovene nickel-molybdenum steel, W. Nr. 1.6587, was used. Its chemical composition is shown in Table 3. The steel is mostly used in the automotive industry. The microstructure formed during the weld thermal cycle application (Figure 6a) was used as an example for the heat treatment in furnace.

The pieces of steel are annealed in the furnace at 1100°C. The grains grow and attain in 3 hours an average size 200 μm. The annealing is followed by cooling in water. The next step of thermal treatment is heating to 870°C and water quenching. The result of this combined thermal treatment, shown in Figure 6b, is pure martensitic coarse-grain microstructure.

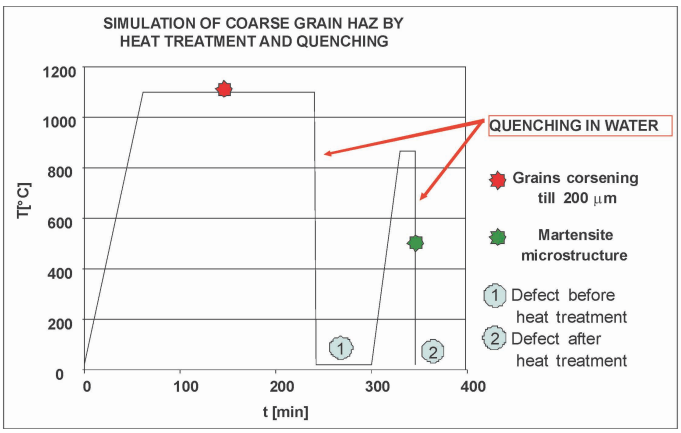

Fig. 5. The heat treatment of the nickel-molybdenum steel using furnace (annealing and quenching)

Table 3.

Chemical composition and properties of the nickel-molybdenum steel

C	Si	Mn	P	S	Cr	Ni	Mo	Cu	Al
mass %									
0.18	0.22	0.43	0.012	0.028	1.56	1.48	0.28	0.15	0.023

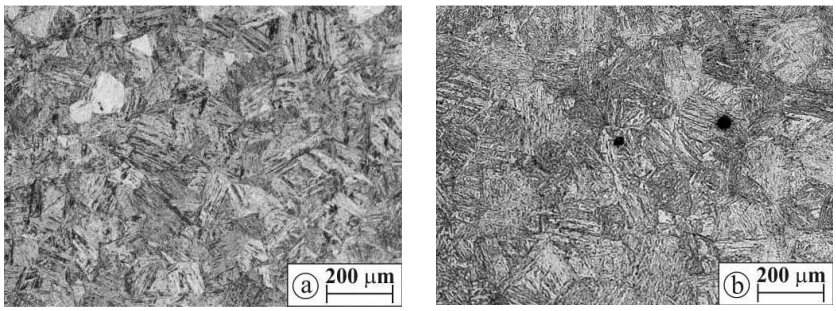

Fig. 6. Microstructure of the coarse-grain steels: a) welding simulation, b) heat treatment in furnace

The rotary bend specimens were machined from the pieces of the steel that was heat treated in the furnace. They were notched in their mid-length (Figure 7).

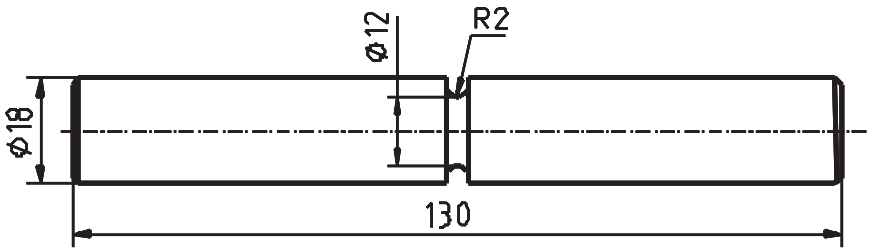

Fig. 7. Geometry of rotary bending specimen

The Vickers indentation is made either before quenching or after quenching (Figure 5: marks 1 and 2). In the case marked as 1, the residual stresses due to indenting are not present and do not affect crack initiation from artificial defects (residual stress free condition), while in the case marked as 2, the residual stresses are present and certainly affect crack initiation (as-indented condition). Besides, the appearance of residual stresses is also linked with changes of the indentation shape.

3. Results and discussion

Smooth and artificially surface-defected specimens shown in Figure 3 with the details at the bottom of the notch shown in Figure 4 were bend-

loaded on a resonant machine at the room temperature in the load-control mode. The frequency of the loading and the stress rate were f ≅ 115 Hz and R ≅ 0, respectively.

The loading was increased in the steps to 2 million cycles, or to fatigue crack initiation, or to the specimen fracture. A new specimen was used each time. The results of the testing are S-N curves valid for test condition C_1-C_6 and different coarse-grain steels M1-M5. The highest stress range, $\Delta\sigma_B$, at which the steel resists after 2 million cycles, is taken as the bending fatigue strength of material, $\Delta\sigma_{f-B}$.

The relationships between the results of the testing expressed as fatigue strength $\Delta\sigma_{f-B}$ and the parameter $\sqrt{area}$ are shown on a logarithmic-logarithmic scale in Figure 8.

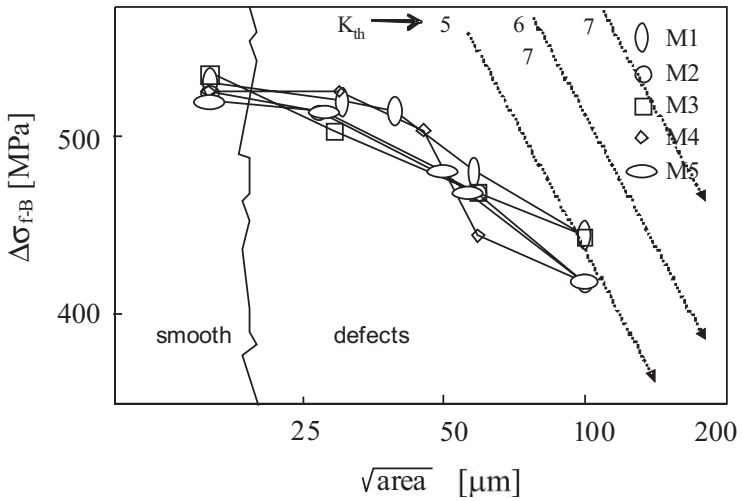

Fig. 8. Bending fatigue strength of five coarse-grained steels versus defect size parameter calculated as illustrated in Figure 4

Smooth and indented specimens (Figure 7) were machined from the pieces of steel that underwent heat treatment in the furnace. The bottom of the notch was ground and polished. The theoretical stress concentration factor caused by the notch is 1.74. An example of the indentation is shown in Figure 9.

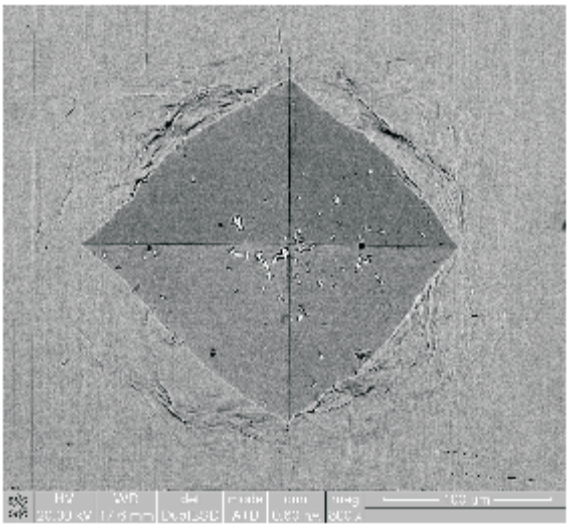

Fig. 9. Vickers indentation with the diagonal 200 μm

The specimens were rotary bend-loaded at the room temperature in the load-control mode. The frequency of the loading and the stress rate were f ≅ 100 Hz and R = -1, respectively. The defect size parameter $\sqrt{area}$ of all indentations was round 53.4 μm.

Loading of the specimens during the tests was constant. When crack initiation was detected in a suitable way [10], the testing was stopped and the specimen was submitted to detailed examination using optical and scanning microscopes. Noticeable striations on the fracture surface did not appear. However, the fracture surface patterns shown in Figure 10 enable us to reveal positions of crack origins. The existence of the radial ledges indicates the direction of crack growth. They can be traced back towards the crack origin.

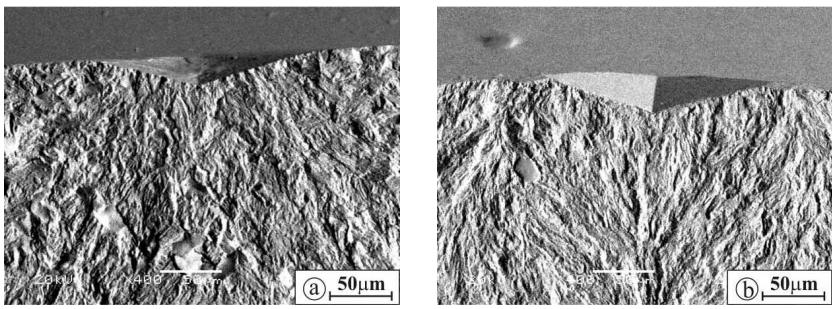

Fig. 10. Fracture surfaces of indented specimens: a) residual stress free condition (crack origin is at the deepest point of the indentation), b) as-indented condition (cracks initiation is at both edges of the indentation)

The pattern of the fracture surface shown in Figure 10a is telling a different story than the pattern shown in Figure 10b. In Figure 10a, the crack initiates at the deepest point of the indentation, and grows in a convex semi-elliptic shape. This is schematically shown in the upper part of Figure 11a. The arrows represent direction of the crack growth from the indentation outwards. This specimen was in the residual stress-free condition, because indenting was performed before the final quenching (Figure 5: mark 1).

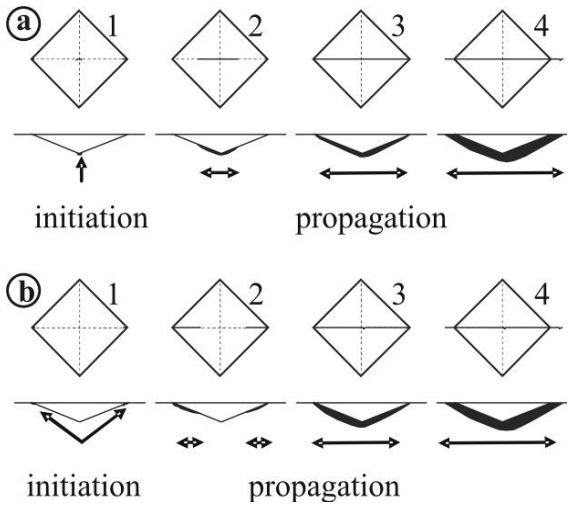

Fig. 11. Four stages of crack initiation and early growth from Vickers indentation: a) residual stress free condition, b) as indented condition

In Figure 10b, two cracks initiate at the edges of the indentation. Their growth and coalescence are schematically shown in the upper part of Figure 11b. The direction of the cracks growth is represented by the attached arrows. In the period of loading time, both cracks coalesce in the middle. During further growth, the crack gradually changes to the expected semi-elliptic shape. This specimen was in the as-indented condition, because indenting was performed after the final quenching (Figure 5: mark 2).

The reason for this specific crack behaviour during the initiation and early crack growth on specimen in the as-indented condition is a compressive residual indenting stress. This stress acts perpendicularly to the edges of the indentation obstructing the crack initiation. The magnitude of the compressive stress is the highest at the deepest point of indentations. Crack initiation at both edges far away from the deepest point of the indentation is easier, because of lower compressive stress.

The correctness of the above-described behaviour in the as-indented condition is proved in the microphotographs of Vickers indentations in the bird's-eye view (Figure 12). Two cracks were initiated a few tens of microns apart

(Figure 12a). At the moment of snap, they were not jointed at the deepest point of the indentation. The next stage in the crack growth is shown in Figure 10b. The cracks are coalesced and already broke to the surface.

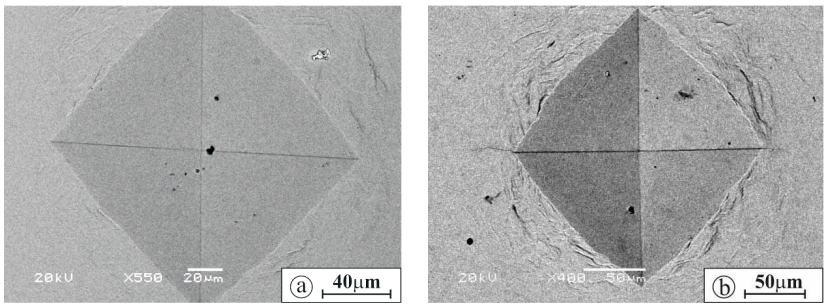

Fig. 12. Two stages of early crack growth on indented specimens in the as-indented condition: a) cracks developed at both edges, b) cracks are already coalesced and spread at the non-indented surface

If the diamond pyramid is assumed to be incompressible and the indented metal ideally plastic, the projection of a Vickers indentation (*area*) will be expressed by using the shape of Vickers pyramid and the measurable size of the indentation on the surface, as shown in Equation 3. Unfortunately, the diamond pyramid is not incompressible, although its elastic modulus is at least 5 times higher than that of steels [11]. The difference is shown in Figure 13. The way of indentation profile measurement is shown elsewhere [10].

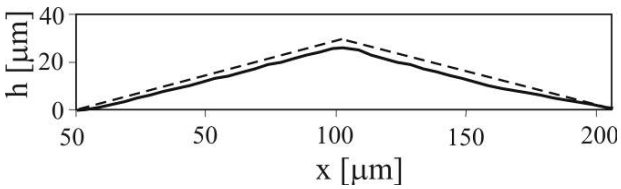

Fig. 13. Profile of the Vickers indentation (dashed line - calculated from the shape of pyramid, solid line - measured)

4. Conclusions

The shape of the curves in Figure 8 complies quite well with the Kitagawa-Takahashy plot. For this reason, three dotted lines are entered in the figure representing possible fatigue strengths of coarse grained HAZ materials with long cracks. One of the lines could be the right-hand side of the Kitagawa-Takahashy plot, because the ΔK_{th}-value for carbon structural steels corresponds to 5-10 MPa $\sqrt{m}$. Unfortunately, actual data for the investigated steels are not available.

The shape of the relationship presenting the dependence of the bending fatigue strength, $\Delta\sigma_{f-B}$, versus the defect size parameter $\sqrt{area}$, shown in Figure 5, does not approach the expected linear trend defined with the assumed three values of DKth-values up to the defect size parameter

On the other hand, it seems that the defect size parameter $\sqrt{area}$ underestimates the fatigue strength lowering the effect of series of indentations. The residual stresses affect crack initiation from artificial defects. In the case of indentations and series of indentations, residual stresses are compressive and very high [10].

It is not possible to conclude what is more important for the unexpected shape of the relationship curve $\Delta\sigma_{f-B} - \sqrt{area}$, the coarse grain size or the residual stresses due to indenting. The length of the biggest series of indentations is almost 700 μm (4-6 time average grain size); the depth of indentations does not exceed 31-32 μm (much less than average grain size). A logical question is, which extension of the series of indentations, length or depth, is more important? The right answer seems to be: that dimension of indentation, in which very high crack initiates.

It was expected that very high specimens in the as-indented condition behave differently that those in the stress-relieved condition. The endurance limit of the specimens in the as-indented condition is 5% lower than that in the stress-relieved condition [10]. The reason is the presence of the residual stresses:

1. When compressive residual stresses are the highest at the deepest point of the indentation, the cracks initiate separately at both loaded edges of indentation. When the stress level is sufficiently low, those cracks become non-propagating after initiation. When stress level is higher, the cracks coalesce at the deepest part of the indentation and create a single crack. The effect of bigger single crack is stronger than the effect of two separate cracks, although its size is almost equal to the sum of lengths of the two cracks.
2. When the residual stresses are not present, cracks initiate as a single crack over the whole length of indentation. An initiated crack in the stress-relieved condition that is longer than the diagonal of indentation has a stronger effect than the effect of two separate cracks in the as-indented condition. Fatigue strength of specimens with very high compressive residual stresses higher than those without very high residual stresses is therefore quite logical.

Generally, compressive stresses at the surface increase the fatigue strength of coarse-grain steels, while the tensile stresses decrease their fatigue strength. In the CGHAZ of welds, the situation is the same.

The testing work has been done and will be continued under the Polish-Slovenian Research Project "Fatigue properties of welded joints in structural steels under exploatation condition" in the years 2008-2009.

Manuscript received by Editorial Board, September 09, 2008;
final version, October 09, 2008.

REFERENCES

[1] Murakami, Y. at al.: Quantitative Evaluation of Effects of Non-Metallic Inclusions on Fatigue Strength of High Strength Steels – I: Basic Fatigue Mechanism and Evaluation of Correlation between the Fatigue Fracture Stress and the Size and Location of Non-Metallic Inclusions, Int. J. of Fatigue, 1989, 9, pp.291-298.
[2] Murakami, Y., Usuki, H.: Quantitative Evaluation of Effects of Non-Metallic Inclusions on Fatigue Strength of High Strength Steels – II: Fatigue Limit Evaluation Based on Statistics for Extreme Values of Inclusion Size, Int. J. of Fatigue, 1989, 9, pp.299-308.
[3] Murakami, Y.: Effects of Small Defects and Nonmetallic Inclusions on Fatigue Strength of Metals, JSME International Journal I, 1989, 32, 2, pp.167-180.
[4] Miller, K. J.: The Behaviour of Short Fatigue Cracks and Their Initiation Part I and Part II, Fatigue Fract. Engng. Mater. Struct., 1987, 10, 1, 75-91 and 2, pp.93-113.
[5] Yasniy P-V. at al.: Microcrack initiation and growth in heat-resistant 15Kh2MFA steel under cyclic deformation, Fatigue Fract. Engng. Mater. Struct., 2005, Vol 28, 4, pp.391-397.
[6] Kitagawa, H., Takahashi, S.: Applicability of Fracture Mechanics to Very Small Cracks or the Cracks in the Early Stage, 2nd International Conference on the Behaviour of Materials, Boston, ZDA, 1976.
[7] Verreman, Y., Bailon, J-P., Masounave, J.: Fatigue Life Prediction of Welded Joints A Re-assessment, Fatigue Fract. Engng. Mater. Struct., 1987, 10, 1, pp.17-36.
[8] Gliha V.: The effect of small flaws on the fatigue strength of HAZ at the weld toe. Int. J. mater. prod. technol., 2007, 29, 1/4, pp.297-310.
[9] Murakami, Y., Endo, M.: Effects of Hardness and Crack Geometries on ΔK_{th} of Small Cracks Emanating from Small Defects, The Behaviour of Short Fatigue Cracks, Edited by K.J.Miller, E.R. de los Rios, Mechanical Engineering Publications, 1986.
[10] Vuherer T.: Analysis of influence of micro defects on the fatigue strength of coarse grain HAZ in welds, Doctoral thesis, University of Maribor, Faculty for Mechanical Engineering, 2008.
[11] Courtney T. H.: Mechanical Behavior of Materials, McGraw-Hill, New York, 1999, pp.59-60.

Modelowanie inicjacji pęknięć zmęczeniowych w strefie wpływu ciepła złącza spawanego

Streszczenie

W pracy dokonano analizy inicjacji pęknięć zmęczeniowych w obrębie defektu powierzchniowego w zamodelowanej strefie wpływu ciepła złącza spawanego elementów ze stali konstrukcyjnej. Próbki z pasmami ziaren o strukturze martenzytycznej wykonano z wykorzystaniem termocyklicznego symulatora spawania oraz pieca laboratoryjnego. Inicjator pękania wykonano w obszarze struktury gruboziarnistej za pomocą wgłębnika twardościomierza Vickersa, uzyskując lokalne spiętrzenie naprężeń. Wielkość uzyskanego odcisku nie przekraczała wielkości pojedynczego ziarna. Badane próbki poddano stałoamplitudowemu zginaniu z częstotliwością f ≅ 115 Hz, przy

współczynniku asymetrii cyklu R ≅ 0. Otrzymane wyniki badań poddano analizie a pracę zakończono wnioskami.